Journal of Cleaner Production 452 (2024) 142172

Contents lists available at ScienceDirect

Journal of Cleaner Production

journal homepage: www.elsevier.com/locate/jclepro

Impact of territorial spatial landscape pattern on $PM_{2.5}$ and O_3 concentrations in the Yangtze River delta urban agglomeration: Exploration and planning strategies☆

Xin Chen *, Fang Wei **

College of Civil Engineering and Architecture, Zhejiang University, Hangzhou, 310058, China

ARTICLE INFO

Handling Editor: Giovanni Baiocchi

Keywords:
$PM_{2.5}$-O_3 composite pollution
Territorial spatial landscape metrics
Variables screening
GTWR
Tradeoff-synergy analysis
Planning strategies

ABSTRACT

$PM_{2.5}$-O_3 composite pollution has become a pressing atmospheric challenge in China. Assessing the impact of territorial spatial landscape pattern on $PM_{2.5}$ and O_3 concentrations within the context of territorial spatial planning will provide ideas for atmospheric governance and spatial planning. Based on the agricultural-urban-ecological space system, this study first reclassifies territorial space within the Yangtze River Delta urban agglomeration (YRDUA) and calculates multilevel and multidimensional landscape metrics. Then, variables are screened by the random forest model and collinearity test. Furthermore, the spatiotemporally heterogeneous impact of selected landscape metrics on $PM_{2.5}$ and O_3 concentrations is explored using the geographically and temporally weighted regression (GTWR) model, with a tradeoff-synergy analysis being conducted to propose planning strategies. The conclusions show: (1) Two pollutant concentrations have both numerical and spatial correlations. The temporal stability of concentrations' responses to metrics is increasing, while the spatial heterogeneity continues to be significant. (2) Aggregation index of agricultural production space (AP_AI) and percentage of forest area (FO_PLAND) are trade-off and synergy factors of coordinated control, respectively. Largest patch index of grassland (GR_LPI) and patch density of other ecological spaces (OT_PD) are individual factors of $PM_{2.5}$ reduction. (3) Spatial zoning supported by intra-zonal and inter-zonal cooperation policies, and coordinated control guidelines centered around the utilization of agricultural production space, have been advocated. This study aims to provide theoretical supplement and practical support for urban agglomeration's atmospheric governance and territorial spatial landscape pattern optimization.

1. Introduction

Air pollution has become increasingly striking in China due to a period of extensive industrialization and rapid urbanization (Duan et al., 2022; Du et al., 2024). In response, the government has launched a series of action plans for cleaner air since 2013. Consequently, among six air pollutants listed by the Ministry of Ecology and Environment of China, SO_2, NO_2, and CO have been effectively controlled, particulate matter concentrations have decreased but are still over-standard, O_3 concentration has been over-standard and continuing to rise (Lin et al., 2022; Tan et al., 2023). This indicates that O_3 and particulate matter, represented by $PM_{2.5}$, have become primary air pollutants (Zhang et al., 2022b; Zhao et al., 2021). $PM_{2.5}$ and O_3 pose risks to public health and living standards, further threatening socio-economic activities (Guan et al., 2021; Liu et al., 2018; Zhang et al., 2017). Therefore, efforts must be taken to control $PM_{2.5}$-O_3 composite pollution in China. In this context, it is necessary to identify factors influencing pollutant concentrations, as well as explore possibilities and strategies for coordinated control.

Existing studies have explored $PM_{2.5}$/O_3 concentrations' correlations with various factors, including meteorological conditions, anthropogenic emissions, socio-economic activities, and territorial spatial pattern (Chen et al., 2023; Lin et al., 2022; Lu et al., 2020; Ma et al., 2023). Among them, territorial space has garnered significant attention because it serves as a carrier of pollutant sources due to human activities (Wu et al., 2021), affects the spatial distribution of pollutants as an

☆ Abbreviation definitions used in the manuscript and their rules are presented in Table S1.

* Corresponding author.
** Corresponding author.
E-mail addresses: 3180104697@zju.edu.cn (X. Chen), weif@zju.edu.cn (F. Wei).

https://doi.org/10.1016/j.jclepro.2024.142172
Received 6 December 2023; Received in revised form 20 March 2024; Accepted 7 April 2024
Available online 10 April 2024

atmospheric underlying surface (Lu et al., 2018), and regulates local microclimate through spatial pattern adjustments (Wang et al., 2018b).

Scholars have initially studied the impact of specific types of territorial space within traditional land-use classifications on pollutant concentrations. Regarding $PM_{2.5}$, existing research finds that construction land is the main source of particle emissions resulting from human activities; Forests and grasslands are typical “sink” spaces that can effectively reduce $PM_{2.5}$ by capturing particles and regulating local microclimate (Cai et al., 2020; Lu et al., 2020; Shen et al., 2023). As for O_3, forests can capture ozone by dry deposition, while simultaneously producing important ozone precursors such as isoprene, so its correlation with O_3 concentration is complicated (Qu et al., 2023; Zhang et al., 2020). Cultivated land usually has relatively high O_3 concentration because nitrogen fertilizers used in cultivation will volatilize, forming nitrogen oxides that promote ozone generation (Duan et al., 2021; Zhu et al., 2019b).

Landscape pattern can indicate various types of spaces within the total territorial space mentioned above, and also detail spatial characteristics such as area, shape, and distribution at both class and landscape levels (Chiang et al., 2021). It influences human activities and atmospheric circulation, thereby affecting the impact of territorial space on the atmospheric environment (Yang et al., 2022; Yoon et al., 2022). Regarding $PM_{2.5}$, at the class level, landscapes with larger area percentages, lower splitting indexes, higher agglomeration indexes, and regular shapes are normally more likely to exert their functions as “source/sink” entities (Lu et al., 2018; Yoon et al., 2022). Accordingly, at the landscape level, a larger percentage of sink space will reduce $PM_{2.5}$ when the aforementioned landscape pattern characteristics are conducive to strengthening the source/sink role of space (Yang et al., 2023b; Zhai et al., 2022b). However, O_3 is a secondary pollutant with a more complex generation mechanism, which determines that its correlation with territorial spatial landscape pattern is uncertain and differs from that of $PM_{2.5}$. For example, Li et al. (2022) found that O_3 in urban areas has increased while $PM_{2.5}$ decreased due to land cover changes in the past two decades in China. Similar findings (Trail et al., 2015; Wu et al., 2021) all indicate the importance of conducting a comparative analysis of $PM_{2.5}$ and O_3 concentrations’ correlations with territorial spatial landscape pattern.

In terms of coordinated control of $PM_{2.5}$-O_3 composite pollution, increasing studies have proposed strategies from the perspective of spatial planning. Existing relevant strategies mainly fall into two categories: spatial zoning and planning guidance. Spatial zoning primarily relies on characteristics of pollutant concentrations and environmental carrying capacity. For example, Yang et al. (2023a) divided China into seven atmospheric governance regions based on spatiotemporal clustering of both $PM_{2.5}$ and O_3 concentrations. Planning guidance is provided merely based on research findings regarding correlations between spatial characteristics and pollutant concentrations (Wu et al., 2021), while consideration of institutional guarantees for its implementation is limited.

Overall, relevant studies still have the following deficiencies: Firstly, territorial space use must be carried out within specific planning contexts. With the adoption of the agricultural-urban-ecological space system framework in China, the traditional land-use classification based on surface cover needs to be transformed into a function-oriented approach. Secondly, existing research mainly focuses on the global impact of territorial spatial landscape pattern on single pollutants, primarily $PM_{2.5}$, lacking analysis of local effects on different pollutants. Thirdly, as for spatial planning strategies, existing spatial zoning lacks a comprehensive basis for zoning and consideration of intra-zonal cooperation, while planning guidance lacks institutional guarantees for implementation.

The Yangtze River Delta urban agglomeration (YRDUA) faces rapid economic development and severe atmospheric pollution, and it also serves as a pioneer for synergistic regional development. To fill research gaps, this study reclassifies the territorial space of 201 counties in the YRUDA into 8 secondary spaces within the agricultural-urban-ecological space system. It calculates and screens landscape metrics by random forest model and collinearity test. Next, geographically and temporally weighted regression (GTWR) is used to analyze the impact of selected metrics on $PM_{2.5}$ and O_3 concentrations, which are then weighed to propose planning strategies. The marginal contribution of this study lies in (1) The pollutants selected and territorial spatial classification framework are better aligned with the practical background of China’s air pollution and spatial planning; (2) The landscape metrics most related to $PM_{2.5}$ and O_3, respectively, are refined by variables screening, and the spatiotemporal heterogeneity of their impacts on pollutant concentrations has been fully explored with GTWR, delving deeper than merely assessing global correlations between various landscape metrics and single pollutant; (3) Building upon existing approaches, several strategies aimed at integrating landscape pattern characteristics control into regional development affairs have been proposed, offering path references for atmospheric governance and spatial planning in urban agglomerations.

2. Materials and methodology

2.1. Study area and period

The Yangtze River Delta urban agglomeration (YRDUA) is located in the middle and lower sections of the Yangtze River within China. It consists of 26 cities as follows: Shanghai (SH); Nanjing (NJ), Wuxi (WX), Changzhou (CZ1), Suzhou (SZ), Nantong (NT), Yancheng (YC), Yangzhou (YZ), Zhenjiang (ZJ), and Taizhou (TZ1) in Jiangsu Province; Hangzhou (HZ1), Ningbo (NB), Jiaxing (JX), Huzhou (HZ2), Shaoxing (SX), Jinhua (JH), Zhoushan (ZS), and Taizhou (TZ2) in Zhejiang Province; Hefei (HF), Wuhu (WH), Ma’anshan (MAS), Tongling (TL), Anqing (AQ), Chuzhou (CZ2), Chizhou (CZ3) and Xuancheng (XC) in Anhui Province.

The YRDUA was chosen as the study area because of its representativeness. Firstly, intensive modernization within the YRDUA has led to a huge conflict between territorial space development and environmental capacity (Gao et al., 2019; Sun et al., 2023). $PM_{2.5}$ and O_3 concentrations in the YRDUA in 2023 remained much higher than the safety value set by the World Health Organization. Secondly, the “Territorial Space Master Plan of the Yangtze River Delta Ecological Green Integration Development Demonstration Zone” was approved in 2023, indicating that the YRDUA needs to strengthen the ecological effect of territorial spatial planning through cross-regional coordination. Additionally, as this study is practical-oriented and spatial big data used is not limited by administrative divisions, 201 counties within 26 cities were selected as basic units (Fig. 1).

Considering that China entered the stage of $PM_{2.5}$-O_3 composite pollution after 2015 (Du et al., 2024) and the availability of official land-use data during this time, this study took 2015, 2018, and 2020 as research periods. Affected by economic transformation and spatial planning adjustments, land cover in China still changed significantly between three selected time points (Kuang et al., 2022), demonstrating its research potential.

2.2. Variables and data

The important section of this study involves employing econometric models to examine the impact of territorial spatial landscape pattern on pollutant concentrations, necessitating the identification of a series of variables. The variables, selected based on research objectives and relevant findings on influencing factors of air quality (Hu et al., 2017; Liu et al., 2022; Lu et al., 2021), are presented in Table 1.

$PM_{2.5}$ concentration data is obtained from the Atmospheric Composition Analysis Group of Washington University in St. Louis (https://sites.wustl.edu/acag/). The dataset is estimated based on the V5. GL.01 algorithm version using data from NASA satellites and ground

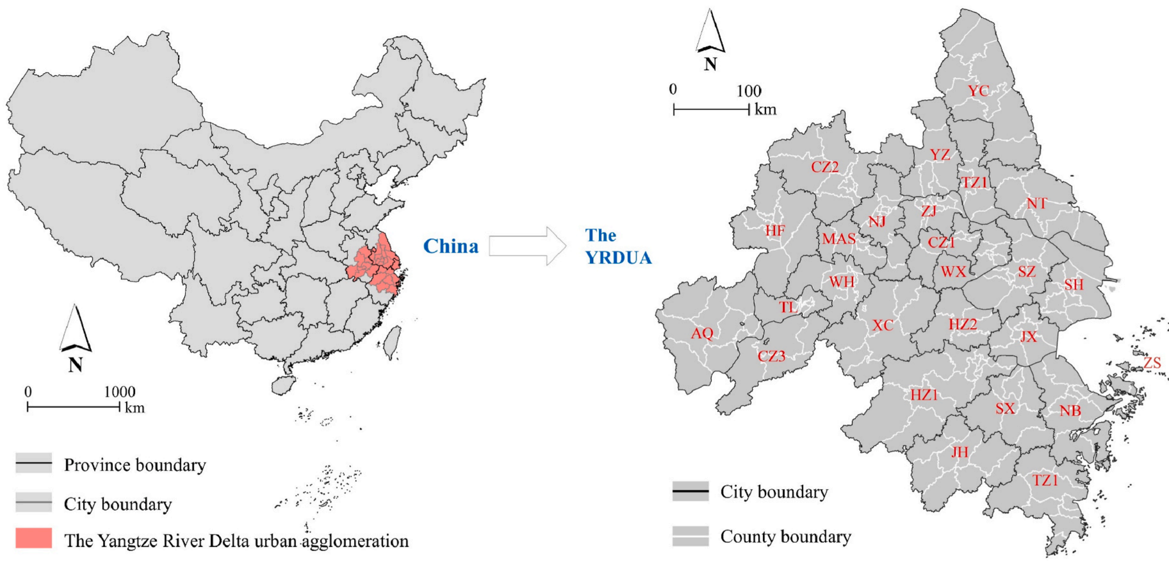

Fig. 1. Location of the YRDUA and research units in it.

Table 1
Variables and detailed indicators.

Variable type	Variable	Indicator	Acronym
Dependent variables	Pollutant concentrations	$PM_{2.5}$ concentration; O_3 concentration	$PM_{2.5}$; O_3
Core explanatory variables	Territorial spatial landscape pattern	Listed in Table 3	
Control variables	Built environment	Road density; NDVI in built-up areas	ROAD; NDVI
	Social-economic factors	GDP; Permanent population density	GDP; POP
	Meteorological factors	Temperature; Precipitation	TEM; PRE

monitoring stations. O_3 concentration data is derived from datasets developed by the Tracking Air Pollution in China (TAP, http://tapdata.org.cn/). TAP calculated data by utilizing machine learning algorithms and fusing multivariate data, and inversion results are highly correlated with the maximum daily average 8-h O_3 concentration monitored on the ground ($R^2 = 0.701$). Land-use data (30 × 30 m) is from the Resource and Environment Data Cloud Platform (https://www.resdc.cn/), which is constructed through manual visual interpretation based on remote sensing images from Landsat Satellite. Road network data is from Gaode Map (https://lbs.amap.com/), we calculated its linear density value after assigning each road its importance value. Normalized Difference Vegetation Index (NDVI) data is from the EARTHDATA Dataset (https://www.earthdata.nasa.gov/). GDP and permanent population data are derived from statistical yearbooks of provinces, cities, and counties. Temperature and precipitation data are obtained from ERA5-Land Dataset (https://cds.climate.copernicus.eu/). County zoning data is from the Resource and Environment Data Cloud Platform (https://www.resdc.cn/).

2.3. Methods

2.3.1. Territorial space reclassification and landscape metrics

Firstly, territorial space was reclassified into three primary spaces (totally owning eight secondary spaces) based on their functional attributes. Among them, agricultural space and urban space primarily accommodate activities for agricultural workers and urban residents, respectively, while ecological space primarily provides various ecological services. Those three spatial functions represent basic human needs and reflect human activities within the space (Li et al., 2023b; Wang et al., 2022), closely related to the generation and reduction of atmospheric pollutants. And they directly depend on land cover characteristics, so the classification standards can be connected to traditional land-use classification (Cao et al., 2022b; Wang et al., 2018a), as formulated in Table 2.

Then, characteristics of secondary spaces' landscape pattern were quantified by landscape metrics, which have been widely used to reflect the composition and spatial characteristics of territorial space (Xiao et al., 2023; Zhang et al., 2022a). According to relevant research (Chiang et al., 2021; Zhang and Zhang, 2021; Zhao and Huang, 2022), metrics at both class and landscape levels were chosen based on three principles: effectively expressing area, shape, distribution, and structure of landscape; ease of calculation and monitoring in practice; applicability to all units. The selected landscape metrics are shown in Table 3, along with their details. All the landscape metrics were calculated using Fragstats 4.2.

2.3.2. Variables screening

Firstly, the random forest (RF) model was used to select the optimal variable set. RF constructs multiple decision trees on the random samples and explanatory variable subsets of the input dataset, then combines the results of decision trees through bootstrapping sampling to provide the best fitting model. RF is capable of quantifying each vari-

Table 2
Territorial space classification connected to traditional land-use classification.

The primary space	The secondary space	Acronym	Land-use type
Agricultural space	Agricultural production space	AP	Paddy land; dry land
	Agricultural living space	AL	Land for rural settlements
Urban space	Urban living space	UL	Urban construction land
	Urban production space	UP	Land for industrial, mining construction, and transportation
Ecological space	Waters	WA	River; Lake; Reservoir; Pond; Glacier; Mudflat; Shoaly land
	Forest	FO	Forest land; Shrub land; Sparse wood; the woodland
	Grassland	GR	High/Moderate/Low coverage grassland
	Other ecological space	OT	Sand land; Marshland; Bare land; Bare rock and gravel land; else

Table 3
Territorial spatial landscape metrics computed in the study.

Metric (Acronym)	Connotation and significance	Class level	Landscape level
Percentage of landscape (PLAND)	The proportion of total landscape area occupied by the calculated landscape class (unit: %). Reflecting the dominance of secondary space to total territorial space.	✓	
Largest patch index (LPI)	The proportion of total landscape area occupied by the largest patch of the calculated landscape class (unit: %). Reflecting the dominance of a single patch within calculated secondary space to total territorial space.	✓	✓
Area weighted mean shape index (AWMSI)	The value of the area-weighted length of all patches' edges divided by the minimum length possible for the same landscape area aggregated maximally (unitless). Reflecting the regularity of patch shape; A larger value means greater complexity.	✓	✓
Edge density (ED)	The total length of all edges of patches per unit area of landscape (unit: m/ha). Reflecting the intensity of interaction between patches; A larger value means greater interaction.	✓	✓
Patch density (PD)	The number of patches per unit area of landscape (unit: 1/ha). Reflecting spatial fragmentation; A larger value means greater fragmentation.	✓	✓
Splitting index (SPLIT)	The number of subdividing the landscape into patches with the same area-weighted mean patch size (unitless). Reflecting spatial separation; A larger value means greater separation.	✓	✓
Contagion (CONTAG)	The tendency of patches to be aggregated (unit: %). Reflecting spatial contagion; A larger value means greater contagion.	✓	✓
Patch cohesion index (COHESION)	The measure of the natural connectivity of patches. Reflecting spatial cohesion; A larger value means greater cohesion.	✓	
Aggregation index (AI)	The number of like adjacencies divided by the maximum possible number of like adjacencies (unit: %). Reflecting spatial aggregation; A larger value means greater aggregation.		✓
Shannon's diversity index (SHDI)	The measure of territorial spatial functional richness in landscape (unitless); A larger value means greater richness.		✓
Shannon's evenness index (SHEI)	The measure of the evenness of patches' areas in landscape (unitless); A larger value means greater evenness.		✓

able's contribution by referring to out-of-bag estimation errors by bootstrapping. So, it could be and has been widely used for variables screening (Wang et al., 2020; Zhao et al., 2023a). Based on the framework proposed by (Yang et al., 2019; Ma et al., 2022), the specific steps in this study are: (1) Perform regression analysis between variables and pollutant concentration using RF, and record out-of-bag score (*OOB_score*) of regression result; (2) Calculate the increase of mean square error (*IncMSE*) of each variable to determine its importance and eliminated the variable with the smallest effect; (3) Redo above steps with remaining variables until no more could be eliminated, select the group of variables with best regression effect (largest *OOB_score*).

Next, the variance inflation factors (*VIF*) of the variables selected above were calculated for collinearity analysis, with final variables being screened by the standard of $VIF < 10$. The formulas are as follows:

$$OOB\_score = 1 - Card[i \in (1, \ldots, n) | y_i \neq \widehat{y_i}] / n \tag{1}$$

$$IncMSE_i = \left(MSE_i^{OOB} - MSE^{OOB}\right) / MSE^{OOB} \tag{2}$$

$$VIF_i = 1 / \left(1 - R_i^2\right) \tag{3}$$

Where $\widehat{y_i}$ is the most frequent label predicted by each tree of the forest (Eq. (1)); MSE^{OOB} is the mean square error of regression result calculated using out-of-bag data in RF, MSE_i^{OOB} is the MSE^{OOB} when feature i is permuted (Eq. (2)); R_i^2 is the coefficient determination of regression result in collinearity test when feature i is treated as dependent variable and regressed with others (Eq. (3)).

2.3.3. Geographically and temporally weighted regression (GTWR) model

As an extension of geographically weighted regression (GWR), GTWR introduces the temporal dimension to consideration of elements' spatial variations. Therefore, it can simultaneously observe both spatial and temporal heterogeneity of correlations between elements (Chen et al., 2021; Ni et al., 2023). The formulas are as follows:

$$Y_i = \beta_0(u_i, v_i, t_i) + \sum_{j=1}^{n} \beta_j(u_i, v_i, t_i) X_{ij} + \varepsilon_i \tag{4}$$

$$\widehat{\beta}(u_i, v_i, t_i) = \left[X^T W(u_i, v_i, t_i) X\right]^{-1} X^T W(u_i, v_i, t_i) Y \tag{5}$$

$$W_{ij} = \exp\left(-d_{ij}^2 / h^2\right), \tag{6}$$

$$d_{ij} = \sqrt{\alpha\left[(u_i - u_j)^2 + (v_i - v_j)^2\right] + \beta(t_i - t_j)^2} \tag{7}$$

In Eq. (4), Y_i and X_{ij} are dependent variable and independent variable j of unit i, respectively; (u_i, v_i, t_i) is the coordinate point (latitude, longitude, time) of unit i; $\beta_j(u_i, v_i, t_i)$ is the estimated coefficient parameters of variable j in unit i, $\beta_0(u_i, v_i, t_i)$ is the intercept parameter; ε_i is the error term.

In Eq. (5), $\widehat{\beta}(u_i, v_i, t_i)$ is the estimated value of $\beta_j(u_i, v_i, t_i)$; $W(u_i, v_i, t_i)$ is the diagonal matrix composited of spatiotemporal weight between various units (W_{ij}, as shown in Eq. (6)), which is calculated by Gaussian kernel function based on spatiotemporal distance between units (d_{ij}, as shown in Eq. (7)).

GTWR calculates interactions between the calculated unit and units within the bandwidth (h), that is, units have different spatiotemporal weight matrixes that are heavily influenced by h. In this study, we adopted the corrected Akashi Information Criterion (AICc) to determine the optimal bandwidth (Huang et al., 2010).

3. Results

3.1. Spatiotemporal characteristics of territorial space

Fig. 2 presents the territorial spatial pattern of the YRDUA in 2015, 2018, and 2020, along with yearly areas of secondary spaces within the agricultural-urban-ecological space system. During study periods, the ratio of agricultural-urban-ecological spaces has remained relatively stable at 5:1:4. Among secondary spaces, agricultural production space owns the largest area, significantly exceeding that of forest and waters (both exceeding 10,000 km^2). Territorial space shows an obvious north-south functional differentiation: Ecological space primarily concentrates in the southern mountainous and hilly area, while a large area of agricultural production space occupies the northern plain area.

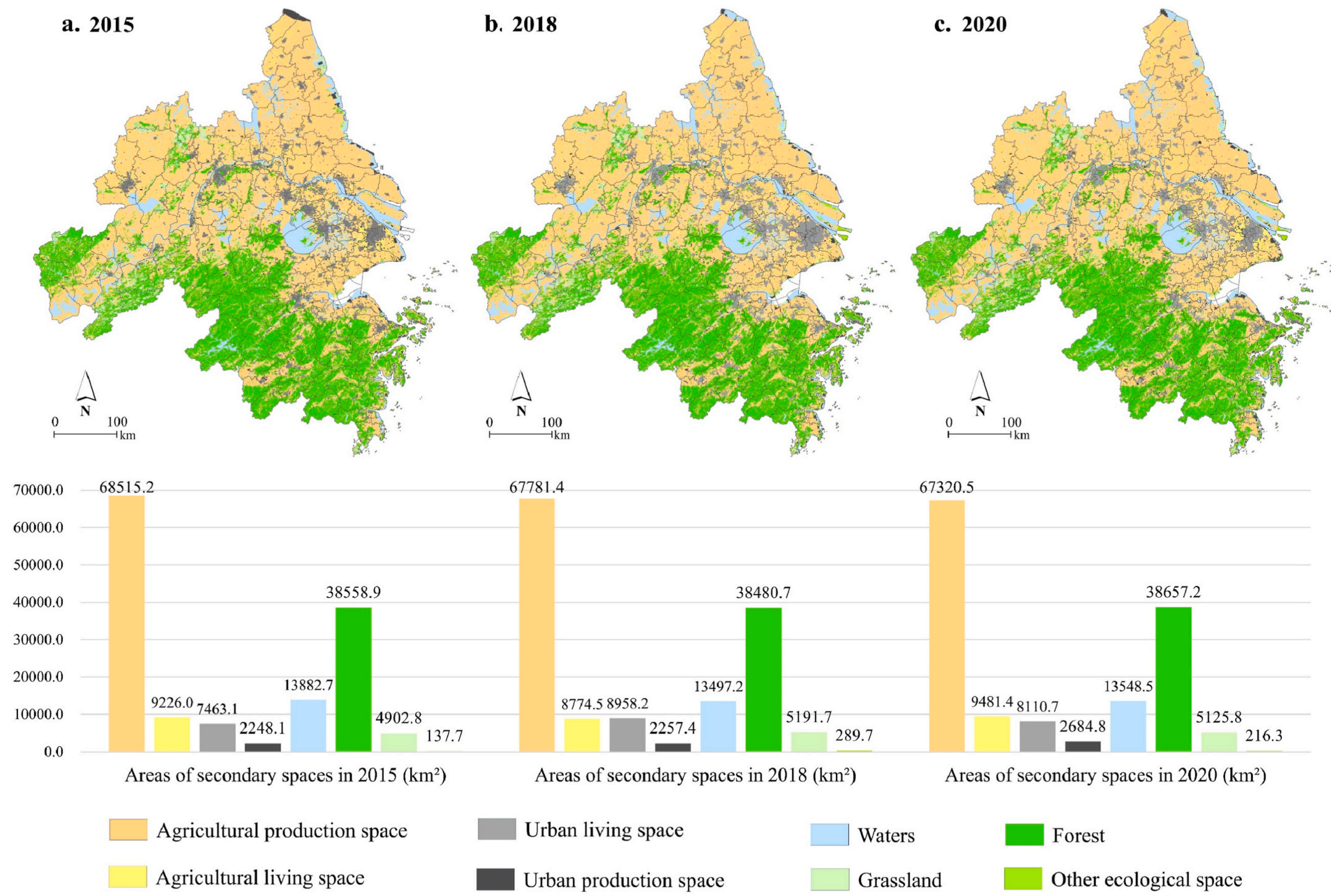

Fig. 2. Territorial spatial pattern and statistics of secondary territorial space area.

3.2. $PM_{2.5}$-O_3 composite pollution characteristics

3.2.1. Spatiotemporal characteristics of $PM_{2.5}$ and O_3 concentrations

Fig. 3 illustrates distributions of pollutant concentrations. During study periods, the numerical level of $PM_{2.5}$ concentration is decreasing, while that of O_3 is increasing. Meanwhile, standard deviations of both $PM_{2.5}$ and O_3 concentrations are decreasing, indicating that pollutant concentrations are increasingly concentrated around the average. Regarding spatial distribution, $PM_{2.5}$ concentration gradually forms a northwest-southeast differentiation pattern, with high values concentrating in Anhui Province and Jiangsu Province, while low values concentrating in Zhejiang Province. O_3 concentration gradually forms a northeast-southwest differentiation pattern, with high values concentrating in Shanghai and Jiangsu Province, while low values concentrating in the southern mountainous and hilly area. The clustering of high-high and low-low pollutant concentrations is consistent with the clustering of urban and ecological spaces, respectively, reflecting the potential impact of territorial spatial pattern on two pollutants.

3.2.2. Numerical correlation between $PM_{2.5}$ and O_3 concentrations

Pearson correlation analysis of $PM_{2.5}$ and O_3 concentrations in research units is made and results are presented in Fig. 4. Positive correlations (0.296, 0.856, 0.677) of $PM_{2.5}$ and O_3 concentrations during study periods have passed significance tests, and the coefficient has reached high (>0.6) since 2018. It indicates that high/low $PM_{2.5}$ concentration is very likely to be accompanied by high/low O_3 concentrations in counties in the YRDUA.

3.2.3. Spatial autocorrelation between $PM_{2.5}$ and O_3 concentrations

Bivariate spatial autocorrelation analysis (Chen and Chi, 2022; Qiao and Huang, 2022) on $PM_{2.5}$ and O_3 concentrations is performed. Regarding global spatial autocorrelation, *Moran's I* indexes are 0.246, 0.754, and 0.610 in 2015, 2018, and 2020, respectively, all passing significance tests. This indicates a significantly positive global spatial correlation between $PM_{2.5}$ and O_3 concentrations during study periods, which has noticeably increased since 2018. As for local spatial autocorrelation (Fig. 5), severe composite pollution areas (high-high clustering) have concentrated in southern Jiangsu Province since 2018, with relatively slight composite pollution areas (low-low clustering) spreading in the core zone of the southern mountainous and hilly area.

3.3. Landscape metrics screening outcomes

Variables (including 9 landscape metrics at the landscape level, 64 landscape metrics at the class level, and 6 control variables) are screened by the RF model, with $PM_{2.5}$ and O_3 concentrations as dependent variables, respectively. When variables are reduced to 8 and 6, regressions of $PM_{2.5}$ and O_3 reach the maximum *OOB_score* respectively (Fig. 6). Further calculation of the collinearity between selected variables shows that the *VIF* of each variable is less than 3, which passed the test (Table 4.

The results show that aggregation index of agricultural production space (AP_AI), percentage of forest area (FO_PLAND), ROAD, TEM, and PRE all have correlations with both $PM_{2.5}$ and O_3 concentrations. Largest patch index of grassland (GR_LPI), patch density of other ecological space (OT_PD), and NDVI are correlated with $PM_{2.5}$ concentration, and GDP is correlated with O_3 concentration. As for

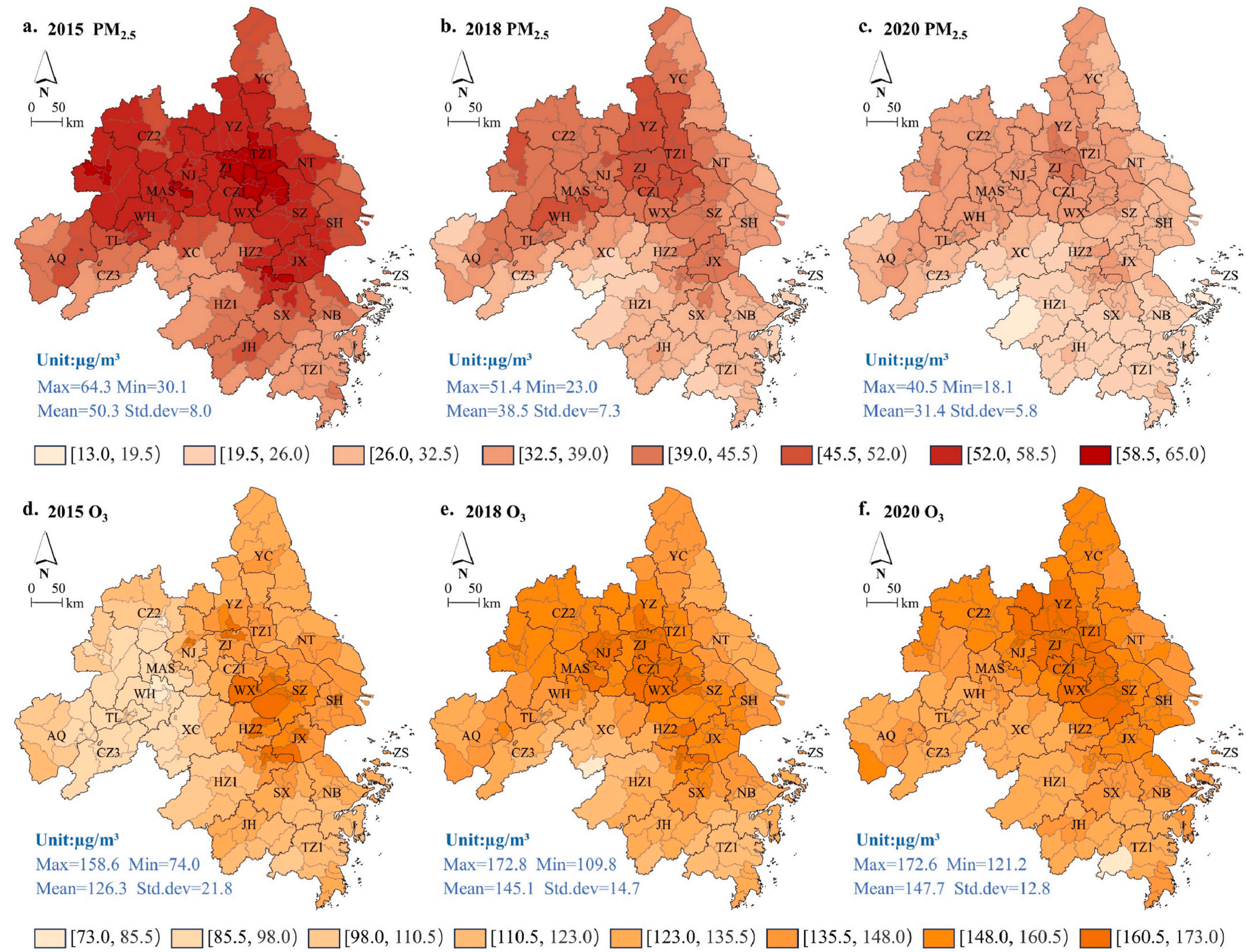

Fig. 3. Spatial distributions of $PM_{2.5}$ and O_3 concentrations.

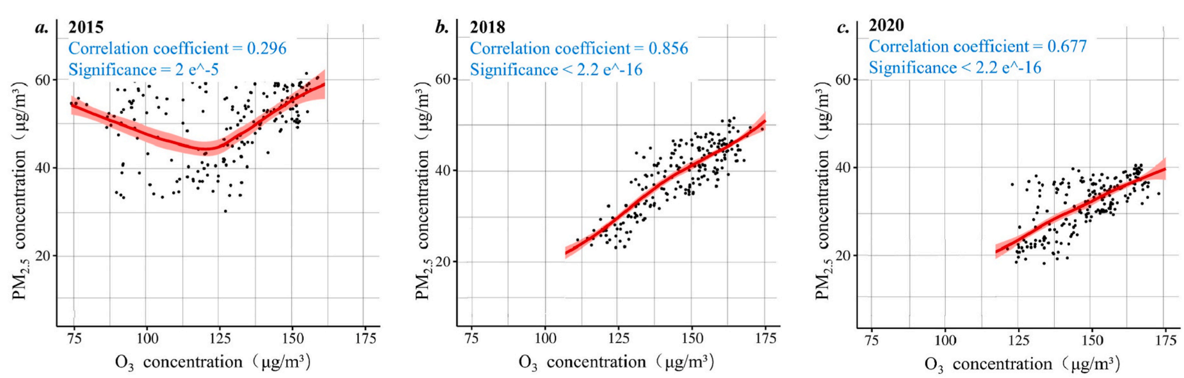

Fig. 4. Correlation (locally weighted) regression charts of $PM_{2.5}$ and O_3 concentrations.

contributions (*IncMSE*) of factors on regression, it can be seen that pollutant concentrations are more directly affected by meteorological and socio-economic factors, while their correlations with landscape metrics are relatively minor. Territorial space serves as the carrier for human production and life, mainly affecting the atmospheric environment by influencing human activities and local microclimate (Cao et al., 2023). Therefore, its relatively indirect impact on air quality and corresponding smaller *IncMSE* make sense. And optimizing territorial spatial pattern remains significantly important in practical atmospheric governance efforts (Wang et al., 2023).

3.4. Estimation results of GTWR model

3.4.1. Performance of regression model

To operate the GTWR model, the spatial autocorrelation of each variable is tested first. The results show that all variables screened have

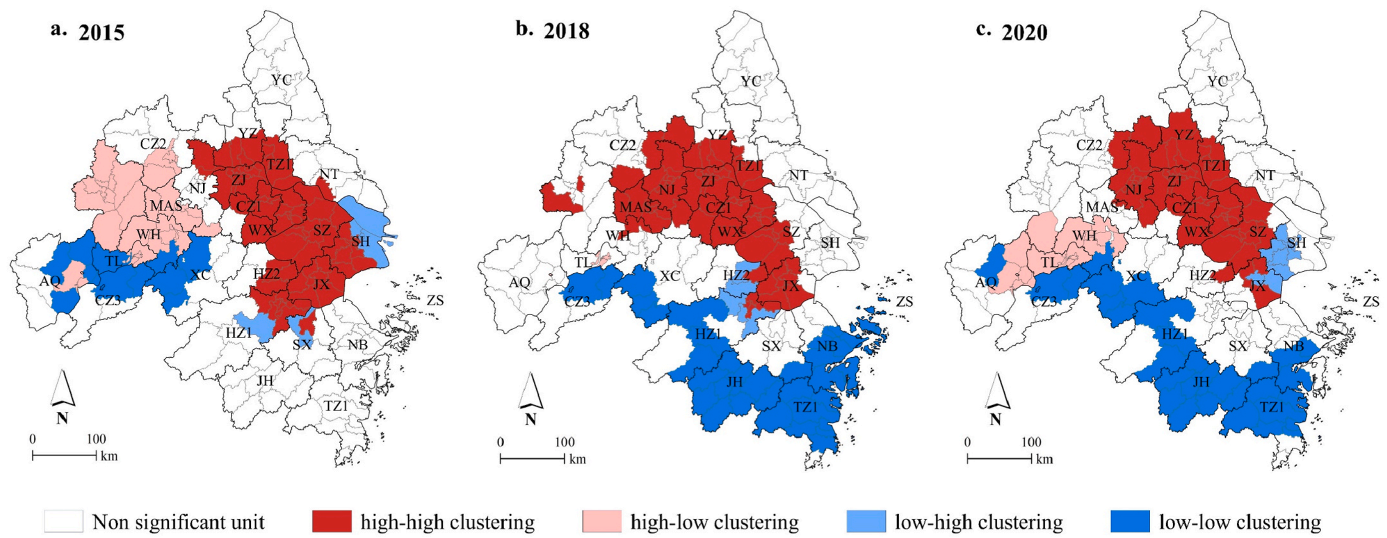

Fig. 5. Spatial clustering of $PM_{2.5}$ and O_3 concentrations by bivariate spatial autocorrelation analysis.

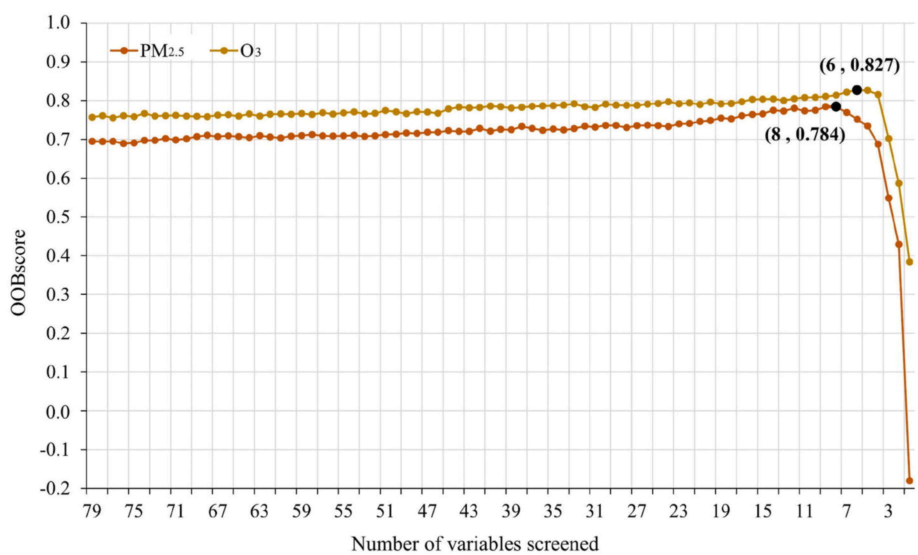

Fig. 6. Number of variables screened iteratively and corresponding *OOB_score* based on RF model.

Table 4
Variables screening outcomes.

Variable	$PM_{2.5}$		O_3	
	IncMSE	*VIF*	*IncMSE*	*VIF*
AP_AI	0.200	1.298	0.371	1.019
FO_PLAND	1.882	1.596	0.557	1.470
GR_LPI	0.134	1.088	–	–
OT_PD	0.243	1.043	–	–
ROAD	1.061	1.352	15.184	1.329
NDVI	0.481	1.537	–	–
GDP	–	–	0.210	1.159
TEM	1.759	1.156	1.102	1.088
PRE	1.118	1.245	0.494	1.210

Note: AP_AI, FO_PLAND, GR_LPI, and OT_PD are landscape metrics at the class level. AP, FO, GR, and OT are types of secondary territorial spaces, as listed in Table 2. AI, PLAND, LPI, and PD are landscape metrics, as listed in Table 3.

spatial autocorrelation and pass significance tests, as listed in Table S2.

Table S3 shows the fitting performance of different regression models. While fitting for $PM_{2.5}$ concentration, GTWR exhibited better results than GWR and ordinary least squares (OLS) models. While fitting for O_3 concentration, GTWR performs significantly better than OLS but slightly inferior to GWR. GTWR comprehensively accounts for spatio-temporal heterogeneity, and its superiority in fitting $PM_{2.5}$ concentration compared to GWR is greater than their difference in fitting O_3 concentration. Therefore, the GTWR model is applied to explain the correlations between variables, with results being visualized as Fig. 7 and 8.

3.4.2. Impacts of landscape metrics on $PM_{2.5}$ concentration

The impact of aggregation index of agricultural production space (AP_AI) on $PM_{2.5}$ concentration shows a pattern of gradually stabilizing planar differentiation. Yancheng (YC) and surrounding counties in the northern YRDUA exhibit sustained small negative coefficients (−0.2~0); The mid-southern YRDUA areas exhibit positive coefficients (0.1~0.2); Anqing (AQ)-Chizhou (CZ3) in the western YRDUA has gradually evolved from negative-correlation areas into strongly positive-correlation areas (0.1~0.5). Areas in the northern YRDUA are characterized by abundant aggregated agricultural production spaces, capable of forming large expanses of pollution-reducing vegetation during crop

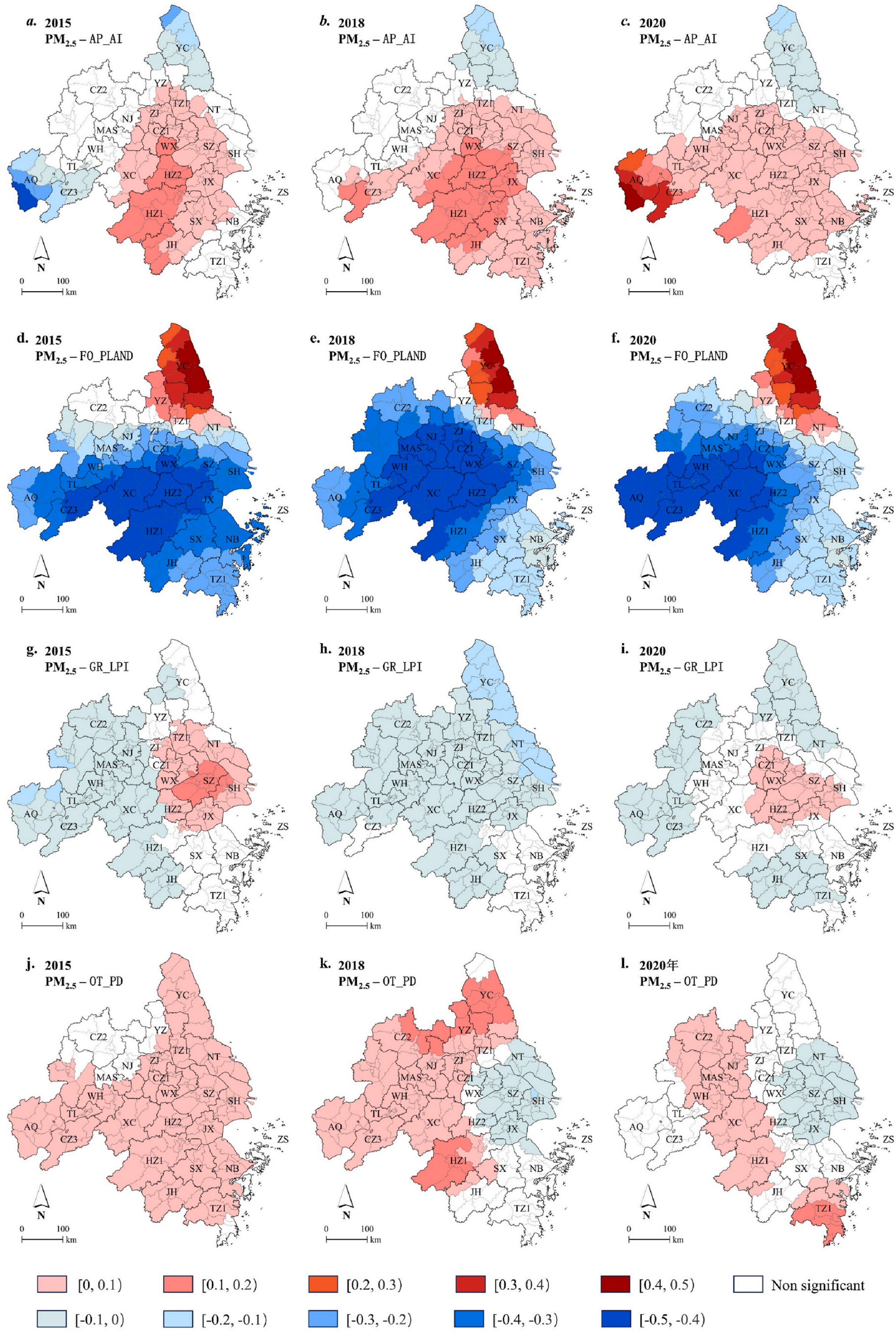

Fig. 7. Spatiotemporal distribution of correlations between screened territorial spatial landscape metrics and $PM_{2.5}$ concentrations.

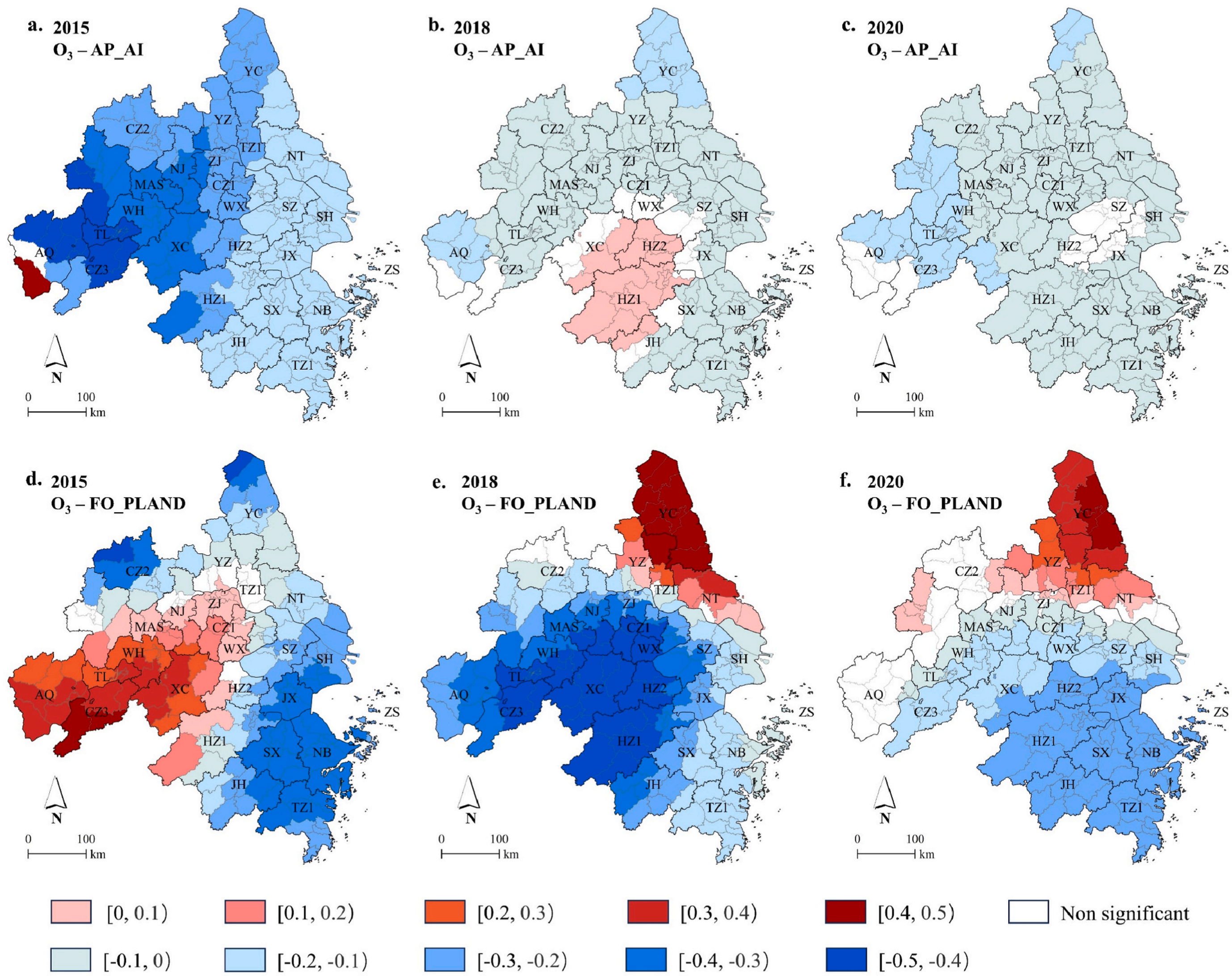

Fig. 8. Spatiotemporal distribution of correlations between screened territorial spatial landscape metrics and O_3 concentrations.

growth (Lu et al., 2020). Territorial space in the mid-southern YRDUA is too fragmented for large-scale agricultural production. Consequently, aggregated agricultural production spaces generate more particles than they capture.

The impact of percentage of forest area (FO_PLAND) on $PM_{2.5}$ concentration consistently covers the entire YRDUA with a strong influence (-0.5~0.5). Yancheng (YC) and surrounding counties exhibit strong positive correlations. The remaining areas exhibit a circular negative-correlation pattern, with the absolute values of coefficients decreasing outward from the high-value core, which gradually shifts from the mid-southern YRDUA to the southwestern YRDUA. Overall, forests with higher coverage, as observed in the southern YRDUA, exhibit a stronger purification effect on $PM_{2.5}$, consistent with the findings of Lin et al. (2020). As the remaining $PM_{2.5}$ for forests to capture decreases, the high-value core of negative-correlation areas shifts. Meanwhile, $PM_{2.5}$ concentration is affected by forest characteristics such as canopy width and leaf area (Liu et al., 2015). Therefore, further analysis is needed to understand situations in positive-correlation areas.

The impact of largest patch index of grassland (GR_LPI) on $PM_{2.5}$ concentration shows instability over time. In 2015, the western YRDUA exhibited negative correlations, while the mid-eastern YRDUA exhibited positive correlations. In 2018, apart from Shaoxing (SX), Ningbo (NB), and Taizhou (TZ2), the YRDUA mainly exhibited negative correlations. In 2020, four significant blocky areas with coefficients concentrating between -0.1 and 0.1 were formed: counties of Anhui Province in the western YRDUA, Yancheng (YC) and surrounding counties, and most counties in the southern Zhejiang Province constituted three negative-correlation areas, while the mid-eastern YRDUA represented the positive-correlation area. Grassland has a similar effect to forests in reducing $PM_{2.5}$ (Xu et al., 2020). Higher GR_LPI in negative-correlation areas indicates a more concentrated distribution of grassland, suggesting its stronger ability to reduce $PM_{2.5}$. In positive-correlation areas, higher GR_LPI indicates a large area of grassland situated far from pollution sources due to the proximity of forests, lakes, and grasslands. Consequently, its ability to reduce pollution is limited, and its positive impact on $PM_{2.5}$ concentration will be amplified due to the disruption of overall spatial continuity.

The impact intensity of patch density of other ecological spaces (OT_PD) on $PM_{2.5}$ concentration mostly falls between -0.1 and 0.1. And the impact area has been shrinking into a blocky differentiation pattern: the axis area from Chuzhou (CZ2) to Hangzhou (HZ1), Taizhou (TZ2) and surrounding counties constitute two positive-correlation areas, while Shanghai (SH)-Suzhou (SZ)-Jiaxing (JX)-Nantong (NT) is identified as the negative-correlation area. Sand land, marshland, bare land, and so on can rarely capture particles; instead, they often serve as sources of particles. Larger OT_PD means a more dispersed distribution of pollutant sources, indicating a weaker ability to reduce $PM_{2.5}$. However, the complex components and evolution mechanisms of these spaces result in a lack of explanation for the observed situations, suggesting the need for further analysis.

3.4.3. Impacts of landscape metrics on O_3 concentration

The range of impact intensity for aggregation index of agricultural production space (AP_AI) on O_3 concentration has shrunk from $-0.5\sim0.5$ to $-0.2\sim0.0$. The impact almost covers the entire YRDUA, with the spatial distribution of coefficients evolving from a band-like decrease from west to east into a globally pancake-shaped pattern. Correlation in the border area between Shanghai (SH), Zhejiang Province, and Anhui Province has experienced fluctuations during study periods. In 2018, Hangzhou (HZ1)-Xuancheng (XC)-Huzhou (HZ2) exhibited positive correlations ($0\sim0.1$), while the surrounding buffer zone showed no correlation. In 2020, the border area of Shanghai (SH)-Suzhou (SZ)-Huzhou (HZ2)-Jiaxing (JX) exhibited no correlation. With many urban spaces and waters existing in this area, an increase in the aggregation of agricultural production spaces will lead to the fragmentation of other spaces, an increase in supporting facilities, and a weakening of the scale effect of forests, making the correlation more complex.

The impact of percentage of forest area (FO_PLAND) on O_3 concentration continues to strongly ($-0.5\sim0.5$) cover the entire YRDUA, with its spatial pattern changing over time. Before 2018, there were enhanced positive correlations towards the southeast and enhanced negative correlations towards the northwest, with Ma'anshan (MAS)-Nanjing (NJ)-Zhenjiang (ZJ)-Wuxi (WX)-Xuancheng (XC) as the boundary. Since then, Yancheng (YC) and surrounding counties have evolved into strong positive-correlation areas, while the remaining areas exhibit negative correlations with values decreasing outward from the high-value core in a circular pattern. That is, despite a large area of forests in the mid-southern YRDUA emitting various volatile organic compounds (VOCs, as ozone precursors), their effect on inhibiting O_3 generation through direct dry deposition of O_3 is more effective (Qu et al., 2023; Yu et al., 2022). The relatively low forest coverage rate in the northern YRDUA prevents the formation of a large pollutant deposition area, allowing VOC emissions to have a greater impact on O_3 (Zhang et al., 2020).

3.4.4. Tradeoff-synergy analysis

Aggregation index of agricultural production space's (AP_AI's) correlations with $PM_{2.5}$ and O_3 concentrations exhibit spatial heterogeneity (exhibiting opposite impacts on two pollutant concentrations in the same units), indicating that it is the trade-off factor of coordinated control. That is, its different impacts on both pollutants should be compared to make decisions in real need. In the northern YRDUA with high coverage of farmland and waters, highly aggregated agricultural production spaces can function similarly to forests during crop growth, thereby reducing $PM_{2.5}$ and O_3 concentrations. In the mid-southern YRDUA, where agricultural production spaces are relatively rare, the aggregated nature of agricultural activities amplifies the positive correlation between crop straw incineration and $PM_{2.5}$ concentration. Agricultural activities do not directly affect O_3, but aggregated agricultural production spaces can reduce the volatilization of NOx in soil and increase the dry deposition rate of O_3. Therefore, although correlations between AP_AI and O_3 concentration fluctuate in the axis area from Hangzhou (HZ1) to Shanghai (SH), the overall trend remains negative.

Percentage of forest area's (FO_PLAND's) correlations with $PM_{2.5}$ and O_3 concentrations exhibit spatial consistency (exhibiting same-direction effects on two pollutant concentrations in the same units), indicating that it is the synergy factor of coordinated control. That is, controlling two pollutants simultaneously could be achieved by adjusting FO_PLAND. Forest exhibits a threshold effect of its area scale on the purification of both pollutants. In the northern YRDUA, agricultural production spaces dominate, with only a small percentage of forest. Therefore, the positive impact on O_3 concentration from forests will likely overweigh the negative impact, while the negative correlation between FO_PLAND and $PM_{2.5}$ concentration might be offset by the effects of other forest characteristics. The high forest coverage rate in the mid-southern YRDUA allows forests to act as a cohesive unit, effectively reducing both pollutants by capturing $PM_{2.5}$ and facilitating the dry deposition of O_3.

4. Discussion

4.1. Feasibility of coordinated governance

Both the synergy of governance objects and the collaboration among governance units are keys to addressing composite pollution, with their feasibility being the prerequisite for coordinated governance. Regarding pollutant objects, $PM_{2.5}$ and O_3 are homologous pollutants with a complex nonlinear chemical coupling relationship (Zhao et al., 2023b; Zhu et al., 2019a). Duan et al. (2022) observed a growing positive correlation between $PM_{2.5}$ and O_3 concentrations in China from 2015 to 2020. The findings of this study align with theirs, indicating that controlling one pollutant can directly influence the other, enabling simultaneous treatment of $PM_{2.5}$ and O_3. In addition, this study further demonstrates the potential for cross-unit collaboration. Consistent with the findings of Lin et al. (2022), the spatial clustering of both $PM_{2.5}$ and O_3 was identified in the study, demonstrating that the impact of atmospheric pollution typically extends across nearby counties. Furthermore, this study calculates the gradual decrease in standard deviations of pollutant concentrations, indicating a convergence in pollution stages faced by each unit. Meanwhile, the spatial autocorrelation between two pollutant concentrations indicates a close relationship between various pollutants in neighboring units. The necessity and feasibility of cross-unit coordinated governance for $PM_{2.5}$ and O_3 have been effectively demonstrated by this study.

4.2. Analysis of the correlation

Previous studies have found that agricultural production space can mimic the pollutant-reducing functions of forests and grasslands during crop growth, while activities like crop burning and mechanical production occurring within it can result in significant dust emissions (Lu et al., 2020). Additionally, agricultural production spaces usually have high O_3 concentrations as sources of nitrogen (Duan et al., 2021). However, this study found that ozone production can be suppressed with increased AP_AI. This can be explained by the findings of Wang et al. (2015) and Cao et al. (2022a): Concentrated agricultural production space can effectively contribute to nitrogen fixation and increase ozone dry deposition rate as a whole system of plants. Meanwhile, this study found that the impact of increased AP_AI on $PM_{2.5}$ is affected by the scale of agricultural production space, with smaller scales magnifying the positive impact of mechanized production more than the negative impact of plants. This explains the wisdom of traditional intensive farming in China and serves as a reminder to reconsider the rationale behind advocating for agricultural mechanization (Daum, 2023) without considering regional differences.

Forest usually has low $PM_{2.5}$ concentration due to its sparse human activities and its ability to adsorb and degrade $PM_{2.5}$ (Nowak et al., 2006; Zheng et al., 2019). Besides, Qiao et al. (2019) found that O_3 precursors in China are more derived from NOx generated by industry and transportation rather than VOCs. Therefore, higher FO_PLAND implies that more forests replace artificial spaces, thereby generating VOCs instead of NOx. As forests reach sufficient scales, their capacity for dry deposition (Yu et al., 2022) can surpass the impact of generated ozone precursors. This explains why afforestation is often regarded and used as an effective way for atmospheric governance. However, the impact of forest can be affected by specific forest characteristics and area scales. For example, Zhai et al. (2022a) found that $PM_{2.5}$ concentration exhibits a negative correlation with canopy density and leaf area index, while also showing a non-linear correlation with the area of roadside forest and landscape forest. Similar patterns are observed in different regions in this study. Therefore, the study proposes that further identification of forest characteristics and scale levels is needed before deciding to enlarge forests in practice.

This study also reveals that GR_LPI and OT_PD are correlated with $PM_{2.5}$ concentration in certain units. Previous studies have found that grassland is usually negatively correlated with $PM_{2.5}$ concentration (Xu et al., 2020), while other ecological spaces, such as sand land and bare land, are normally sources of particles (Wu et al., 2015). However, limited research has explored the impact of their landscape pattern on $PM_{2.5}$ concentration. Based on research results, this study proposes that the spatial location of grassland and other ecological spaces will have a stronger impact on pollutant concentrations than the influence of landscape pattern alone, given that they comprise relatively small percentages of the total territorial space. When grassland is situated near pollution sources, higher GR_LPI indicates a more concentrated distribution, contributing to its effectiveness. When other ecological spaces are situated far from pollution sources, lower OT_PD implies that these spaces are more aggregated and thereby easier to manage.

Additionally, based on the GTWR results, the impact of territorial spatial landscape pattern on pollutant concentrations exhibited significant spatial heterogeneity, with the spatial distribution of impact gradually stabilizing over time. However, the findings of Fu et al. (2022) in Heilongjiang Province, China, differ from ours. There, the temporal heterogeneity of meteorological factors' impact on $PM_{2.5}$ concentration was significantly stronger than the spatial heterogeneity from 2014 to 2018. This could be attributed to the slower variability of territorial space compared to meteorological conditions, indicating that managing territorial space is relatively easier than adjusting meteorological conditions. Therefore, it is a feasible approach to address atmospheric pollution through a stable and continuously implemented territorial spatial plan.

4.3. Planning strategies

Implement dynamic monitoring of territorial space using technological tools such as remote sensing and geographic information system, and integrate landscape metrics control into spatial planning and regional development initiatives. China has experienced several phases of atmospheric governance, with the initial strategy of end-of-emission management witnessing diminishing marginal benefits. At this juncture, optimizing the territorial spatial landscape pattern can provide an effective supplement (Li et al., 2023a). However, existing policies regarding territorial space use typically focus on area metrics, suggesting a need to incorporate a broader range of landscape metrics into management affairs. For example, AP_AI can be included as an environmental assessment item, and farmers can receive ecological compensation for achieving higher AP_AI.

Develop guidelines for the coordinated control of composite pollution, emphasizing the tailored utilization of agricultural production space based on local conditions. Unlike GR_LPI and OT_PD, which only have a local impact on $PM_{2.5}$ concentration, the impact of AP_AI and FO_PLAND on both $PM_{2.5}$ and O_3 concentrations generally covers the entire YRDUA. Among them, although the impact intensity of FO_PLAND is the greatest, it diminishes over time, reflecting the decreasing marginal benefits of afforestation for air purification. Meanwhile, agriculture production space takes the largest area percentage of territorial space, and its landscape pattern is crucial for food security, thereby receiving increasing attention in China in recent years (Qiu et al., 2020). Furthermore, adjusting the area of a specific territorial space by changing its boundary is challenging in practice, while focusing on spatial layout forms of specific space is more feasible. Therefore, in the long term, controlling composite pollution by optimizing territorial spatial landscape pattern can primarily be achieved by adjusting the landscape morphology of agricultural production space, with a focus on its aggregation. In detail, according to the findings of this study, the decision to adopt continuous large-scale production or fragmentally dispersed utilization of agricultural production space should be aligned with regional conditions.

Conduct spatial zoning based on multiple factors and provide policy support for intra-zonal and inter-zonal cooperation. The territorial spatial landscape pattern exhibits significant spatial heterogeneity in its impacts on pollutant concentrations. Neighboring counties exhibit strong overall characteristics, indicating the need for a joint multi-county zoning scale to implement differentiated strategies. Therefore, the study proposes that cross-county control zones with differentiated planning strategies for optimizing territorial spatial landscape pattern could be piloted, based on current composite pollution status, territorial spatial characteristics, impacts of landscape metrics on air quality, and regional cooperative bases. Furthermore, incorporating the territorial space landscape pattern characteristics as ecological products into intra-zonal management and inter-zonal trading should be considered, enhancing the feasibility of zoning planning.

Formulate a guarantee institution to promote the implementation of the aforementioned planning and policies. For governments, several approaches can be taken as follows: Strengthen cooperation among stakeholder departments by establishing working groups; Implement an accountability mechanism to enhance regulatory enforcement of governments. Meanwhile, several approaches can be taken to stimulate public awareness and participation as follows: Popularize information about the correlation between territorial space and the atmospheric environment; Publicize regional territorial spatial planning and special plans for atmospheric governance; Take incentive mechanisms to promote grassroots supervision over important territorial space such as forests and agricultural production spaces.

5. Conclusions

This study focuses on $PM_{2.5}$-O_3 composite pollution from the perspective of territorial spatial planning. Landscape metrics of eight secondary spaces within the agricultural-urban-ecological space system are calculated, followed by screening using RF and collinearity tests. Subsequently, correlations between screened metrics and two pollutant concentrations are examined, along with the exploration of potential planning strategies. The major conclusions could be summarized as follows: (1) The decrease in standard deviations of both $PM_{2.5}$ and O_3 concentrations over time, along with their correlation in numerical level and spatial distribution, demonstrate the necessity for coordinated control of composite pollution. (2) The sets of landscape metrics screened with $PM_{2.5}$ and O_3 concentrations respectively have overlapping components. Their spatial heterogeneity in impacts on pollutant concentrations remains significant, with temporal heterogeneity decreasing. (3) The impact of AP_AI and FO_PLAND on $PM_{2.5}$ and O_3 concentrations follows a planar spatial pattern, and further analysis reveals that they are trade-off and synergistic factors of composite pollution, respectively. GR_LPI and OT_PD are individual factors for $PM_{2.5}$ pollution control, with their impact distributed in a blocky pattern. (4) The study proposes incorporating landscape metrics control into regional development efforts. Specifically, it advocates for making coordinated control guidelines centered around the utilization of agricultural production space, as well as conducting spatial zoning based on multiple factors combined with intra-zonal and inter-zonal cooperation policies.

Still, several limitations also exist. Firstly, constrained by data availability, only two-dimensional planar landscape metrics were selected to quantify territorial spatial landscape pattern. Subsequent research could take three-dimensional landscape metrics as a supplement. Secondly, although this study quantified and further qualitatively analyzed correlations between territorial spatial landscape pattern and pollutant concentrations, it did not reflect the true causalities of them. Further research could address this gap by combining methods such as structural causal models and machine learning.

CRediT authorship contribution statement

Xin Chen: Writing – review & editing, Writing – original draft, Software, Methodology, Formal analysis, Data curation, Conceptualization. **Fang Wei:** Writing – review & editing, Supervision.

Declaration of competing interest

The authors declare that they have no known competing financial interests or personal relationships that could have appeared to influence the work reported in this paper.

Data availability

Data will be made available on request.

Appendix A. Supplementary data

Supplementary data to this article can be found online at https://doi.org/10.1016/j.jclepro.2024.142172.

References

Cai, L., Zhuang, M., Ren, Y., 2020. A landscape scale study in Southeast China investigating the effects of varied green space types on atmospheric PM2.5 in mid-winter. Urban For. Urban Green. 49, 126607 https://doi.org/10.1016/j.ufug.2020.126607.

Cao, J., Chang, M., Pan, Y., Song, T., Liu, Z., Zhao, H., Zhou, M., Zhang, L., Wang, X., 2022a. Assessment and intercomparison of ozone dry deposition schemes over two ecosystems based on Noah-MP in China. Atmos. Environ. 290, 119353 https://doi.org/10.1016/j.atmosenv.2022.119353.

Cao, J., Pan, G., Zheng, B., Liu, Y., Zhang, G., Liu, Y., 2023. Significant land cover change in China during 2001–2019: implications for direct and indirect effects on surface ozone concentration. Environ. Pollut. 335, 122290 https://doi.org/10.1016/j.envpol.2023.122290.

Cao, Y., Jiang, Y., Feng, L., Shi, G., He, H., Yang, J., 2022b. Identification of territorial spatial pattern conflicts in Aksu River Basin, China, from 1990 to 2020. Sustainability 14, 14941. https://doi.org/10.3390/su142214941.

Chen, C., Gao, B., Xu, M., Liu, S., Zhu, D., Yang, J., Chen, Z., 2023. The spatiotemporal variation of PM2.5-O3 association and its influencing factors across China: dynamic Simil-Hu lines. Sci. Total Environ. 880, 163346 https://doi.org/10.1016/j.scitotenv.2023.163346.

Chen, W., Chi, G., 2022. Urbanization and ecosystem services: the multi-scale spatial spillover effects and spatial variations. Land Use Pol. 114, 105964 https://doi.org/10.1016/j.landusepol.2021.105964.

Chen, Y., Tian, W., Zhou, Q., Shi, T., 2021. Spatiotemporal and driving forces of Ecological Carrying Capacity for high-quality development of 286 cities in China. J. Clean. Prod. 293, 126186 https://doi.org/10.1016/j.jclepro.2021.126186.

Chiang, L.-C., Wang, Y.-C., Chen, Y.-K., Liao, C.-J., 2021. Quantification of land use/land cover impacts on stream water quality across Taiwan. J. Clean. Prod. 318, 128443 https://doi.org/10.1016/j.jclepro.2021.128443.

Daum, T., 2023. Mechanization and sustainable agri-food system transformation in the Global South. A review. Agron. Sustain. Dev. 43, 16. https://doi.org/10.1007/s13593-023-00868-x.

Du, S., He, C., Zhang, L., Zhao, Y., Chu, L., Ni, J., 2024. Policy implications for synergistic management of PM2.5 and O3 pollution from a pattern-process-sustainability perspective in China. Sci. Total Environ. 916, 170210 https://doi.org/10.1016/j.scitotenv.2024.170210.

Duan, W., Wang, X., Cheng, S., Wang, R., 2022. Regional division and influencing mechanisms for the collaborative control of PM2.5 and O3 in China: a joint application of multiple mathematic models and data mining technologies. J. Clean. Prod. 337, 130607 https://doi.org/10.1016/j.jclepro.2022.130607.

Duan, Z., Yang, Y., Wang, L., Liu, C., Fan, S., Chen, C., Tong, Y., Lin, X., Gao, Z., 2021. Temporal characteristics of carbon dioxide and ozone over a rural-cropland area in the Yangtze River Delta of eastern China. Sci. Total Environ. 757, 143750 https://doi.org/10.1016/j.scitotenv.2020.143750.

Fu, L., Wang, Q., Li, J., Jin, H., Zhen, Z., Wei, Q., 2022. Spatiotemporal heterogeneity and the key influencing factors of PM2.5 and PM10 in Heilongjiang, China from 2014 to 2018. Int. J. Environ. Res. Publ. Health 19, 11627. https://doi.org/10.3390/ijerph191811627.

Gao, J., Yu, Z., Wang, L., Vejre, H., 2019. Suitability of regional development based on ecosystem service benefits and losses: a case study of the Yangtze River Delta urban agglomeration, China. Ecol. Indicat. 107, 105579 https://doi.org/10.1016/j.ecolind.2019.105579.

Guan, Y., Xiao, Y., Wang, F., Qiu, X., Zhang, N., 2021. Health impacts attributable to ambient PM2.5 and ozone pollution in major Chinese cities at seasonal-level. J. Clean. Prod. 311, 127510 https://doi.org/10.1016/j.jclepro.2021.127510.

Hu, D., Wu, J., Tian, K., Liao, L., Xu, M., Du, Y., 2017. Urban air quality, meteorology and traffic linkages: Evidence from a sixteen-day particulate matter pollution event in December 2015, Beijing. J. Environ. Sci., Climate Change and Urban Environment 59, 30–38. https://doi.org/10.1016/j.jes.2017.02.005.

Huang, B., Wu, B., Barry, M., 2010. Geographically and temporally weighted regression for modeling spatio-temporal variation in house prices. Int. J. Geogr. Inf. Sci. 24, 383–401. https://doi.org/10.1080/13658810802672469.

Kuang, W., Zhang, S., Du, G., Yan, C., Wu, S., Li, R., Lu, D., Pan, T., Ning, J., Guo, C., Dong, J., Bao, Y., Chi, W., Dou, Y., Hou, Y., Yin, Z., Chang, L., Yang, J., Xie, J., Qiu, J., Zhang, H., Zhang, Y., Yang, S., Sa, R., Liu, J., 2022. Monitoring periodically national land use changes and analyzing their spatiotemporal patterns in China during 2015–2020. J. Geogr. Sci. 32, 1705–1723. https://doi.org/10.1007/s11442-022-2019-0.

Li, J., Han, L., Zhou, W., Li, W., Qian, Y., Zhang, Z., 2023a. Uncertainties in research between urban landscape and air quality: summary, demonstration, and expectation. Landsc. Ecol. 38, 2475–2485. https://doi.org/10.1007/s10980-023-01744-5.

Li, L., Huang, X., Yang, H., 2023b. Scenario-based urban growth simulation by incorporating ecological-agricultural-urban suitability into a Future Land Use Simulation model. Cities 137, 104334. https://doi.org/10.1016/j.cities.2023.104334.

Li, L., Zhu, A., Huang, L., Wang, Q., Chen, Y., Ooi, M.C.G., Wang, M., Wang, Y., Chan, A., 2022. Modeling the impacts of land use/land cover change on meteorology and air quality during 2000–2018 in the Yangtze River Delta region. China. Sci. Total Environ. 829, 154669 https://doi.org/10.1016/j.scitotenv.2022.154669.

Lin, H., Zhu, J., Jiang, P., Cai, Z., Yang, Xinyu, Yang, Xiaohui, Zhou, Z., Wei, J., 2022. Assessing drivers of coordinated control of ozone and fine particulate pollution: Evidence from Yangtze River Delta in China. Environ. Impact Assess. Rev. 96, 106840 https://doi.org/10.1016/j.eiar.2022.106840.

Lin, Y., Yang, X., Li, Y., Yao, S., 2020. The effect of forest on PM2.5 concentrations: a spatial panel approach. For. Policy Econ. 118, 102261 https://doi.org/10.1016/j.forpol.2020.102261.

Liu, H., Liu, S., Xue, B., Lv, Z., Meng, Z., Yang, X., Xue, T., Yu, Q., He, K., 2018. Ground-level ozone pollution and its health impacts in China. Atmos. Environ. 173, 223–230. https://doi.org/10.1016/j.atmosenv.2017.11.014.

Liu, M., Wei, D., Chen, H., 2022. Consistency of the relationship between air pollution and the urban form: Evidence from the COVID-19 natural experiment. Sustain. Cities Soc. 83, 103972 https://doi.org/10.1016/j.scs.2022.103972.

Liu, X., Yu, X., Zhang, Z., 2015. PM2.5 concentration differences between various forest types and its correlation with forest structure. Atmosphere 6, 1801–1815. https://doi.org/10.3390/atmos6111801.

Lu, D., Mao, W., Yang, D., Zhao, J., Xu, J., 2018. Effects of land use and landscape pattern on PM2.5 in Yangtze River Delta, China. Atmos. Pollut. Res. 9, 705–713. https://doi.org/10.1016/j.apr.2018.01.012.

Lu, D., Xu, J., Yue, W., Mao, W., Yang, D., Wang, J., 2020. Response of PM2.5 pollution to land use in China. J. Clean. Prod. 244, 118741 https://doi.org/10.1016/j.jclepro.2019.118741.

Lu, J., Li, B., Li, H., Al-Barakani, A., 2021. Expansion of city scale, traffic modes, traffic congestion, and air pollution. Cities 108, 102974. https://doi.org/10.1016/j.cities.2020.102974.

Ma, S., Kumakoshi, Y., Koizumi, H., Yoshimura, Y., 2022. Determining the association of the built environment and socioeconomic attributes with urban shrinking in Yokohama City. Cities 120, 103474. https://doi.org/10.1016/j.cities.2021.103474.

Ma, X., Yin, Z., Cao, B., Wang, H., 2023. Meteorological influences on co-occurrence of O3 and PM2.5 pollution and implication for emission reductions in Beijing-Tianjin-Hebei. Sci. China Earth Sci. 66, 1258–1267. https://doi.org/10.1007/s11430-022-1070-y.

Ni, F., Wang, Q., Shao, W., Zhang, J., Shan, Y., Sun, X., Guan, Q., 2023. Spatiotemporal characteristics and driving mechanisms of PM10 in arid and semi-arid cities of northwest China. J. Clean. Prod. 419, 138273 https://doi.org/10.1016/j.jclepro.2023.138273.

Nowak, D.J., Crane, D.E., Stevens, J.C., 2006. Air pollution removal by urban trees and shrubs in the United States. Urban For. Urban Green. 4, 115–123. https://doi.org/10.1016/j.ufug.2006.01.007.

Qiao, W., Huang, X., 2022. The impact of land urbanization on ecosystem health in the Yangtze River Delta urban agglomerations, China. Cities 130, 103981. https://doi.org/10.1016/j.cities.2022.103981.

Qiao, X., Wang, P., Zhang, J., Zhang, H., Tang, Y., Hu, J., Ying, Q., 2019. Spatial-temporal variations and source contributions to forest ozone exposure in China. Sci. Total Environ. 674, 189–199. https://doi.org/10.1016/j.scitotenv.2019.04.106.

Qiu, L., Zhu, J., Pan, Y., Wu, S., Dang, Y., Xu, B., Yang, H., 2020. The positive impacts of landscape fragmentation on the diversification of agricultural production in Zhejiang Province, China. J. Clean. Prod. 251, 119722 https://doi.org/10.1016/j.jclepro.2019.119722.

Qu, Y., Wang, T., Yuan, C., Wu, H., Gao, L., Huang, C., Li, Y., Li, M., Xie, M., 2023. The underlying mechanisms of PM2.5 and O3 synergistic pollution in East China: Photochemical and heterogeneous interactions. Sci. Total Environ. 873, 162434 https://doi.org/10.1016/j.scitotenv.2023.162434.

Shen, Z., Zhang, Z., Cui, L., Xia, Z., Zhang, Y., 2023. Coordinated change of PM2.5 and multiple landscapes based on spatial coupling model: Comparison of inland and waterfront cities. Environ. Impact Assess. Rev. 102, 107194 https://doi.org/10.1016/j.eiar.2023.107194.

Sun, B., Fang, C., Liao, X., Guo, X., Liu, Z., 2023. The relationship between urbanization and air pollution affected by intercity factor mobility: a case of the Yangtze River Delta region. Environ. Impact Assess. Rev. 100, 107092 https://doi.org/10.1016/j.eiar.2023.107092.

Tan, S., Xie, D., Ni, C., Zhao, G., Shao, J., Chen, F., Ni, J., 2023. Spatiotemporal characteristics of air pollution in Chengdu-Chongqing urban agglomeration (CCUA) in Southwest, China: 2015–2021. J. Environ. Manag. 325, 116503 https://doi.org/10.1016/j.jenvman.2022.116503.

Trail, M., Tsimpidi, A.P., Liu, P., Tsigaridis, K., Hu, Y., Nenes, A., Stone, B., Russell, A.G., 2015. Reforestation and crop land conversion impacts on future regional air quality in the Southeastern U.S. Agric. For. Meteorol. 209–210, 78–86. https://doi.org/10.1016/j.agrformet.2015.05.001.

Wang, D., Fu, J., Xie, X., Ding, F., Jiang, D., 2022. Spatiotemporal evolution of urban-agricultural-ecological space in China and its driving mechanism. J. Clean. Prod. 371, 133684 https://doi.org/10.1016/j.jclepro.2022.133684.

Wang, J., He, T., Lin, Y., 2018a. Changes in ecological, agricultural, and urban land space in 1984–2012 in China: land policies and regional social-economical drivers. Habitat Int. 71, 1–13. https://doi.org/10.1016/j.habitatint.2017.10.010.

Wang, R., Asghari, V., Hsu, S.-C., Lee, C.-J., Chen, J.-H., 2020. Detecting corporate misconduct through random forest in China's construction industry. J. Clean. Prod. 268, 122266 https://doi.org/10.1016/j.jclepro.2020.122266.

Wang, W., Wang, C., Sardans, J., Min, Q., Zeng, C., Tong, C., Peñuelas, J., 2015. Agricultural land use decouples soil nutrient cycles in a subtropical riparian wetland in China. Catena 133, 171–178. https://doi.org/10.1016/j.catena.2015.05.003.

Wang, X., Tian, G., Yang, D., Zhang, W., Lu, D., Liu, Z., 2018b. Responses of PM2.5 pollution to urbanization in China. Energy Pol. 123, 602–610. https://doi.org/10.1016/j.enpol.2018.09.001.

Wang, Y., Wang, M., Wu, Y., Sun, G., 2023. Exploring the effect of ecological land structure on PM2.5: a panel data study based on 277 prefecture-level cities in China. Environ. Int. 174, 107889 https://doi.org/10.1016/j.envint.2023.107889.

Wu, J., Li, J., Peng, J., Li, W., Xu, G., Dong, C., 2015. Applying land use regression model to estimate spatial variation of PM2.5 in Beijing, China. Environ. Sci. Pollut. Res. 22, 7045–7061. https://doi.org/10.1007/s11356-014-3893-5.

Wu, J., Wang, Y., Liang, J., Yao, F., 2021. Exploring common factors influencing PM2.5 and O3 concentrations in the Pearl River Delta: Tradeoffs and synergies. Environ. Pollut. 285, 117138 https://doi.org/10.1016/j.envpol.2021.117138.

Xiao, H., Luo, Y., Jiang, M., Su, R., Li, J., Xiang, R., Hu, R., 2023. Landscape patterns are the main regulator of pond water chlorophyll α concentrations in subtropical agricultural catchments of China. J. Clean. Prod. 425, 139013 https://doi.org/10.1016/j.jclepro.2023.139013.

Xu, G., Ren, X., Xiong, K., Li, L., Bi, X., Wu, Q., 2020. Analysis of the driving factors of PM2.5 concentration in the air: a case study of the Yangtze River Delta, China. Ecol. Indicat. 110, 105889 https://doi.org/10.1016/j.ecolind.2019.105889.

Yang, C., Zhan, Q., Lv, Y., Liu, H., 2019. Downscaling land surface temperature using multiscale geographically weighted regression over heterogeneous landscapes in wuhan, China. IEEE J. Sel. Top. Appl. Earth Obs. Rem. Sens. 12, 5213–5222. https://doi.org/10.1109/JSTARS.2019.2955551.

Yang, H., Leng, Q., Xiao, Y., Chen, W., 2022. Investigating the impact of urban landscape composition and configuration on PM2.5 concentration under the LCZ scheme: a case study in Nanchang, China. Sustain. Cities Soc. 84, 104006 https://doi.org/10.1016/j.scs.2022.104006.

Yang, J., Chen, X., Li, M., Yao, Q., Lv, Q., Gao, B., Chen, Z., 2023a. The division of PM2.5-O3 composite airborne pollution across China based on spatiotemporal clustering. J. Clean. Prod. 401, 136706 https://doi.org/10.1016/j.jclepro.2023.136706.

Yang, L., Wang, S., Hu, X., Shi, T., 2023b. County-based PM2.5 concentrations' prediction and its relationship with urban landscape pattern. Processes 11, 704. https://doi.org/10.3390/pr11030704.

Yoon, S., Heo, Y., Park, C.-R., Kang, W., 2022. Effects of landscape patterns on the concentration and recovery time of PM2.5 in South Korea. Land 11, 2176. https://doi.org/10.3390/land11122176.

Yu, J., Zhou, W., Wu, J., Li, X., Liu, S., Wang, R., Liu, L., Jiang, Q., Tie, X., Li, G., 2022. Impacts of changes in land use and land cover between 2001 and 2018 on summertime O3 formation in North China Plain and surrounding areas–A case study. J. Geophys. Res. Atmospheres 127, e2021JD035956. https://doi.org/10.1029/2021JD035956.

Zhai, C., Bao, G., Zhang, D., Sha, Y., 2022a. Urban forest locations and patch characteristics regulate PM2.5 mitigation capacity. Forests 13, 1408. https://doi.org/10.3390/f13091408.

Zhai, H., Yao, J., Wang, G., Tang, X., 2022b. Impact of land use on atmospheric particulate matter concentrations: a case study of the Beijing–Tianjin–Hebei region, China. Atmosphere 13, 391. https://doi.org/10.3390/atmos13030391.

Zhang, F., Chen, Y., Wang, W., Jim, C.Y., Zhang, Z., Tan, M.L., Liu, C., Chan, N.W., Wang, D., Wang, Z., Rahman, H.A., 2022a. Impact of land-use/land-cover and landscape pattern on seasonal in-stream water quality in small watersheds. J. Clean. Prod. 357, 131907 https://doi.org/10.1016/j.jclepro.2022.131907.

Zhang, J., Wang, J., Sun, Y., Li, J., Ninneman, M., Ye, J., Li, K., Crandall, B., Mao, J., Xu, W., Schwab, M.J., Li, W., Ge, X., Chen, M., Ying, Q., Zhang, Q., Schwab, J.J., 2022b. Insights from ozone and particulate matter pollution control in New York City applied to Beijing. Npj Clim. Atmospheric Sci. 5, 1–7. https://doi.org/10.1038/s41612-022-00309-8.

Zhang, W., Zhang, J., 2021. Scaling effects on landscape metrics in alpine meadow on the central Qinghai-Tibetan Plateau. Glob. Ecol. Conserv. 29, e01742 https://doi.org/10.1016/j.gecco.2021.e01742.

Zhang, X., Du, J., Zhang, L., Huang, T., Gao, H., Mao, X., Ma, J., 2020. Impact of afforestation on surface ozone in the North China Plain during the three-decade period. Agric. For. Meteorol. 287, 107979 https://doi.org/10.1016/j.agrformet.2020.107979.

Zhang, Xin, Zhang, Xiaobo, Chen, X., 2017. Happiness in the air: How does a dirty sky affect mental health and subjective well-being? J. Environ. Econ. Manag. 85, 81–94. https://doi.org/10.1016/j.jeem.2017.04.001.

Zhao, B., Deng, M., Shi, Y., 2023a. Inferring nonwork travel semantics and revealing the nonlinear relationships with the community built environment. Sustain. Cities Soc. 99, 104889 https://doi.org/10.1016/j.scs.2023.104889.

Zhao, H., Chen, K., Liu, Z., Zhang, Y., Shao, T., Zhang, H., 2021. Coordinated control of PM2.5 and O3 is urgently needed in China after implementation of the "Air pollution prevention and control action plan.". Chemosphere 270, 129441. https://doi.org/10.1016/j.chemosphere.2020.129441.

Zhao, X., Huang, G., 2022. Urban watershed ecosystem health assessment and ecological management zoning based on landscape pattern and SWMM simulation: a case study of Yangmei River Basin. Environ. Impact Assess. Rev. 95, 106794 https://doi.org/10.1016/j.eiar.2022.106794.

Zhao, X., Zhang, Z., Xu, J., Gao, J., Cheng, S., Zhao, Xiaoxi, Xia, X., Hu, B., 2023b. Impacts of aerosol direct effects on PM2.5 and O3 respond to the reductions of different primary emissions in Beijing-Tianjin-Hebei and surrounding area. Atmos. Environ. 309, 119948 https://doi.org/10.1016/j.atmosenv.2023.119948.

Zheng, Y., Li, S., Zou, C., Ma, X., Zhang, G., 2019. Analysis of PM2.5 concentrations in Heilongjiang Province associated with forest cover and other factors. J. For. Res. 30, 269–276. https://doi.org/10.1007/s11676-018-0640-7.

Zhu, J., Chen, L., Liao, H., Dang, R., 2019a. Correlations between PM2.5 and ozone over China and associated underlying reasons. Atmosphere 10, 352. https://doi.org/10.3390/atmos10070352.

Zhu, Z., Wang, G., Dong, J., 2019b. Correlation analysis between land use/cover change and air pollutants—a case study in Wuyishan city. Energies 12, 2545. https://doi.org/10.3390/en12132545.